MYCOSPHERE 16(1): 2576–2598 (2025) www.mycosphere.org ISSN 2077 7019
Doi 10.5943/mycosphere/16/1/15

ARTICLE

Epidemiology, risk factors and virulence analysis of *Candida* infection in Southwest China

Wang D[1], Wang C[1,2], Wang YY[1,3], Pan WH[4], Luo G[1], Huang XH[5], Xue WW[6], Nie L[7], Chen CB[5,6*] and Kang YQ[1*]

[1] *Guizhou Key Laboratory of Microbio and Infectious Disease Prevention & Control, Joint Laboratory of Shanghai Dongli One Health Research Institute Co., Ltd. and Guizhou Medical University One Health Research Institute, Guizhou Medical University, Guiyang 561113, P.R. China*

[2] *Reproductive Medicine Center, Guiyang Maternal and child Health Care Hospital & Guiyang children's Hospital, Guiyang 550003, P.R. China*

[3] *Department of infection management, Affiliated Hospital of Guizhou Medical University, Guiyang 550004, P.R. China*

[4] *Department of Dermatology, Shanghai Key Laboratory of Medical Mycology, Changzheng Hospital, Naval Medical University, Shanghai 200003, P.R. China*

[5] *Unit of Pathogenic Fungal Infection & Host Immunity, CAS Key Laboratory of Molecular Virology and Immunology, Shanghai Institute of Immunity and Infection, Chinese Academy of Sciences, Shanghai 200031, P.R. China*

[6] *Nanjing Advanced Academy of Life and Health, Nanjing 211100, P.R. China*

[7] *Department of Laboratory Medicine, The First People's Hospital of Foshan, Foshan 528000, P.R. China*

Citation – Wang D, Wang C, Wang YY, Pan WH, Luo G, Huang XH, Xue WW, Nie L, Chen CB and Kang YQ 2025 – Epidemiology, risk factors and virulence analysis of *Candida* infection in Southwest China. Mycosphere 16(1), 2576–2598, Doi 10.5943/mycosphere/16/1/15

Abstract

Fungal infections, especially invasive candidiasis caused by *Candida* species, have been shown to increase mortality rates among critically ill patients. However, there remains a dearth of epidemiological data on invasive *Candida* infections in Southwest China. This retrospective study sought to address this gap by investigating species distribution, underlying diseases, and risk factors among hospitalized patients with confirmed *Candida* infections in hospitals of Southwest China from 2019-2023. Additionally, we systematically analyzed the virulence properties of strains isolated from different clinical sources and action of cytokines involved in inflammatory and immune responses. A total of 4662 patients were included in the present study, with 174 identified as having bloodstream infection. Our data revealed that *Candida albicans* was the predominant infecting organism. Univariate analysis showed significant differences in ICU admission, respiratory dysfunction, solid tumors, neurological disorders, and gastrointestinal pathology between patients with *C. albicans* infections and those with non-*albicans Candida* infections. Multivariate analysis demonstrated that non-*albicans Candida* species are common pathogens in central venous catheter associated bloodstream infections [OR (2.488; 95% CI, 1.043-5.934)]. The invasive virulence determinants of the clinical *Candida* strains were also determined *in vitro* and *in vivo* (*Galleria mellonella* and murine models). And cytokine profiles in mice with *C. albicans* infections varied by the source of the isolate.

Submitted: 24 April 2025; **Accepted:** 18 July 2025; **Published:** 30 July 2025
***Corresponding Authors:** cbchen@siii.cas.cn (C.B. Chen); kangyingqian@gmc.edu.cn (Y.Q. Kang).
Accepted by: Masoomeh Shams-Ghahfarokhi

The prevalence of non-*albicans Candida* infections in Southwest China is progressively rising annually, exacerbated by underlying comorbidities in infected individuals. Thus, our work underscores the significance of prompt identification, diagnosis and management of *Candida* infections in clinical practice.

Keywords – bloodstream infection – candidiasis – cytokine profiles – epidemiology – risk factors – virulence

INTRODUCTION

Candida, as opportunistic pathogens, colonize the human body and can cause a range of infections, from superficial mucosal afflictions to severe systemic candidiasis (Govrins et al. 2023). The global rise in the number of immunocompromised individuals has precipitated a significant increase in the incidence of *Candida* infections, thereby exacerbating morbidity, mortality, and healthcare costs (Koehler et al. 2019). Specifically, *Candida albicans* (*C. albicans*) has been prominently documented in global literatures (Shiori et al. 2023). Recent studies highlight a worldwide increase in non-*albicans Candida* (NAC) species, such as *Nakaseomyces glabrata* (*N. glabrata,* formerly *Candida glabrata*), *Candida parapsilosis* (*C. parapsilosis*), and *Candida tropicalis* (*C. tropicalis*) on an international scope (Sunil et al. 2022). This epidemiological shift emphasizes the need for a thorough understanding of *Candida* infections.

Additionally, regional variations in the prevalence of *Candida* infections are evident (Guo et al. 2013). The significant challenge posed by *Candida* infections in Southwest China is linked to the region's unique ecological, demographic, and socioeconomic traits, yet the paucity of epidemiological data accentuates the necessity for more research into local epidemiological patterns (Zeng et al. 2019). The region's population includes a significant number of individuals from many minority groups, which can restrict access to healthcare and heighten vulnerability to infections. A retrospective study reported a high prevalence of transfusion-transmittable infections (TTIs) among blood donors in Southwest China, highlighting broader public health challenges in the region (Xu et al. 2018). Environmental conditions in Southwest China, such as those influencing soil-transmitted helminths (STH) infections, may also affect the spread of fungal infections like candidiasis (Liu et al. 2015). These findings underscore the need for comprehensive public health strategies that address both medical and socioeconomic determinants of health to effectively combat *Candida* infections and improve overall health outcomes in Southwest China. Moreover, a range of risk factors associated with *Candida* infection has been identified across diverse populations, encompassing conventional factors such as the use of broad-spectrum antibiotics, the presence of indwelling medical devices, and immunosuppression (Silvia et al. 2017). However, these factors may manifest distinctive patterns in Southwest China, owing to the region's unique healthcare beliefs, cultural practices, and genetic predispositions among the ethnic minorities.

Despite the well-recognized prevalence and importance of *Candida* infections, the variability in virulence and pathogenicity among strains from diverse sample origins remains insufficiently studied (Feng et al. 2024). The site of infection can significantly impact the expression of virulence in *Candida* strains, which may be influenced by a spectrum of genetic backgrounds, phenotypic characteristics, and adaptations of the host immune system adaptations (Ruan et al. 2014). This article aims to provide a contemporaneous analysis of the epidemiology, risk factors, and pathogenic

features of various *Candida* strains in Southwestern China, with the intension of establishing foundational insights for the comprehensive management and prevention of candidiasis both within China and globally.

MATERIALS AND METHODS

Study design and setting

A retrospective study was carried out at general hospitals in Southwest China: the Affiliated Dazu Hospital of Chongqing Medical University, Qingzhen First People's Hospital, and Nanchong Central Hospital, covering hospitalizations between from January 2019 to October 2023. The study focused on patients with *Candida* infections, collecting data on demographic profiles and baseline clinical features, including age, gender, infection type, sample origin, inpatient department, and potential comorbidities. Multiple risk factors associated with candidemia were evaluated, including age over 60 years, central venous catheters, other types of catheters, mechanical ventilation, parenteral nutrition, surgical procedures, ICU stays, antimicrobial administration, and corticosteroid therapy. The diagnosis of *Candida* infection and candidemia was made in accordance with the Candidiasis Management Guidelines established by the Chinese Medical Association and the Infectious Diseases Society of America (Keighley et al. 2021).

Experimental animals and strains

Female BALB/c mice (6-12 weeks old) were obtained from Beijing Vitong Lihua Experimental Animal Technology Co., Ltd. Final-instar *Galleria mellonella* larvae, each weighing approximately 200 - 250 mg, were used (Herculano et al. 2024). The larvae were raised at room temperature. Forty-five *C. albicans* strains were isolated from various clinical sources: sputum, vaginal secretions, oral swabs, urine, wound exudate, skin, blood, digestive fluids, and ascites, with five strains obtained from each source. Twenty non-*albicans Candida* strains included *Candida tropicalis*, *Nakaseomyces glabrata*, *Candida parapsilosis*, and *Candida krusei*, with five strains for each species. For *in vivo* screening in mice, 18 clinical *C. albicans* isolates (two per source) were included, obtained from nine anatomical sites (such as sputum and blood) to ensure pathogen diversity. All experimental strains selected in this study were all confirmed by molecular identification of the ITS region, with specific results detailed in Supplementary Table S1.

In vitro detection of virulence factors

Production of phospholipase and proteinase was assayed by inoculating 5 μL aliquots of *Candida* suspensions (10^7 CFU/mL, prepared from overnight YPD cultures at 30°C) onto bovine serum albumin medium (for proteinase) and egg yolk emulsion medium (for phospholipase), followed by incubation at 37 °C for 5–10 days. Enzymatic activity was quantified by measuring the colony diameter and hydrolytic halo diameter to calculate the Pz value (Pz = colony diameter / [colony diameter + halo diameter]), where lower Pz values indicate higher enzymatic activity. Hyphal formation ability was assessed by inoculating single *Candida* colonies into YPD medium for overnight culture at 30 °C, preparing suspensions at 5×10^5 CFU/mL, and adding 40 μL aliquots to each well of a 96 well plate. The total volume per well was adjusted to 200 μL using Spider medium. Samples were incubated at 37 °C for 4 h to induce hyphae, followed by quantification of hyphal cells under an inverted microscopy (count per 100 randomly selected cells). For biofilm production

detection, *Candida* colonies were cultured overnight in YPD medium at 30 °C, transferred to RPMI 1640 (OD_{600} = 0.5), and seeded in 96-well plates (200 μL/well). After 90-min of adhesion (37 °C, 250 rpm), supernatants were removed, wells were washed with PBS, and 200 μL fresh RPMI 1640 was added. Plates were sealed and incubated for 24 h (37 °C, 250 rpm). Biofilms were washed 3 times with PBS, then reacted with 200 μL of PBS containing 12 μL XTT-menadione solution (1 mg/mL XTT: 0.4 mM menadione = 1:5) for 2 h (37 °C, protected from light). The absorbance (OD_{490}) of 100 μL supernatant was measured.

Fungal infection and phenotypic analysis of animals

Sixty-five *Candida* strains from different sources were cultured in Yeast Extract Peptone Dextrose Medium (YPD) at 30 °C with shaking at 200 rpm for 12-16 hours. A suspension of 2×10^5 CFU/mL was prepared for the infection experiments. BALB/c mice were divided into 10 groups following the principles of randomization, control and double-blindness, with 10 mice per group. The mice were then infected via tail vein with 200 μL of the *C. albicans* suspension, and their survival and tissue fungal burden were monitored. *C. albicans* is known to specifically target the kidneys in systemic infections, especially in murine models. This tropism is supported by studies showing that mice infected with *C. albicans* exhibit a significant fungal burden in the kidneys, often resulting in severe histological abnormalities and increased mortality (Frank et al. 2018). Three days after infection, the mice were euthanized under anesthesia to harvest kidney tissues and collect blood samples. The kidneys were weighed and homogenized in 1 mL of PBS using a tissue homogenizer. Serial dilutions were prepared, and appropriate dilutions were plated on Sabouraud Dextrose Agar Medium (SDA). Following 48 hours of incubation at 30 °C, colonies were enumerated to assess the tissue fungal burden. The collected mouse blood was incubated for 30 minutes, after which serum was separated by centrifuging at 3000-5000 × g for 10-15 minutes. The concentrations of IL-2, IL-4, IL-10, and IL-7A in the serum were quantified using commercial ELISA kits, in accordance with the manufacturer's instructions. *Galleria mellonella* larvae were divided into 65 groups, with 20 individuals per group. Each larva was injected with a 10 μL inoculum of *C. albicans* into the right first ventral proleg. After injection, the larvae were incubated at 37 °C. Mortality of *Galleria mellonella* was monitored at 24-hour intervals over a 7-day period. Larvae were considered dead if they exhibited a darkened body and no response to external stimuli.

Statistical analyses

Data analyses were conducted using SPSS software (version 24 for Windows). Continuous variables were presented as mean ± standard deviation (SD) or median with interquartile range, depending on their distribution. Categorical variables were analyzed using Chi-square tests or two-tailed Fisher's exact tests for analysis. Univariate and multivariate analyses were used to evaluate the influencing factors distinguishing between *C. albicans* and NAC infections.

Ethical approval

It was provided by the Experimental Ethics Committee of Shanghai Institude of Immunity and Infection Chinese Academy of Sciences (CAS-2023-034), the Affiliated Dazu Hospital of Chongqing Medical University (CQMU-2024-096), Qingzhen First People's Hospital (QZPH-2024-038), and

Nanchong Central Hospital (NCCH-2024-101), following the standards of the Declaration of Helsinki.

RESULTS

Clinical characteristics of *Candida* infections (Figs 1–5, Table 1)

Over the course of the five-year study, a total of 4662 patients were included, and 174 were diagnosed as having bloodstream infection. The study identified 21 distinct *Candida* species (Fig. 1A). *C. albicans* was the most prevalent species, followed in frequency by *Nakaseomyces glabrata*, *Candida tropicalis*, *Candida parapsilosis*, and *Candida krusei*. Within the patient cohort diagnosed with *Candida* bloodstream infection (BSI), nine unique *Candida* species were identified (Fig. 1B), namely *C. albicans*, *C. tropicalis*, *C. parapsilosis*, *N. glabrata*, *Candida famata* (*C. famata*), *Candida krusei* (*C. krusei*), *Candida dubliniensis* (*C. dubliniensis*), *Candida guilliermondii* (*C. guilliermondii*), and *Candida rugosa* (*C. rugosa*). The highest incidence was observed in 2022 in the patient population diagnosed with *Candida* infections. In the cohort of BSI patients, the peak incidence was recorded in 2023, with 2021 and 2020 reporting the lowest rates (Fig. 2). Notably, the incidence of NAC infections outstripped that of *C. albicans* in the years 2023, 2022 and 2020.

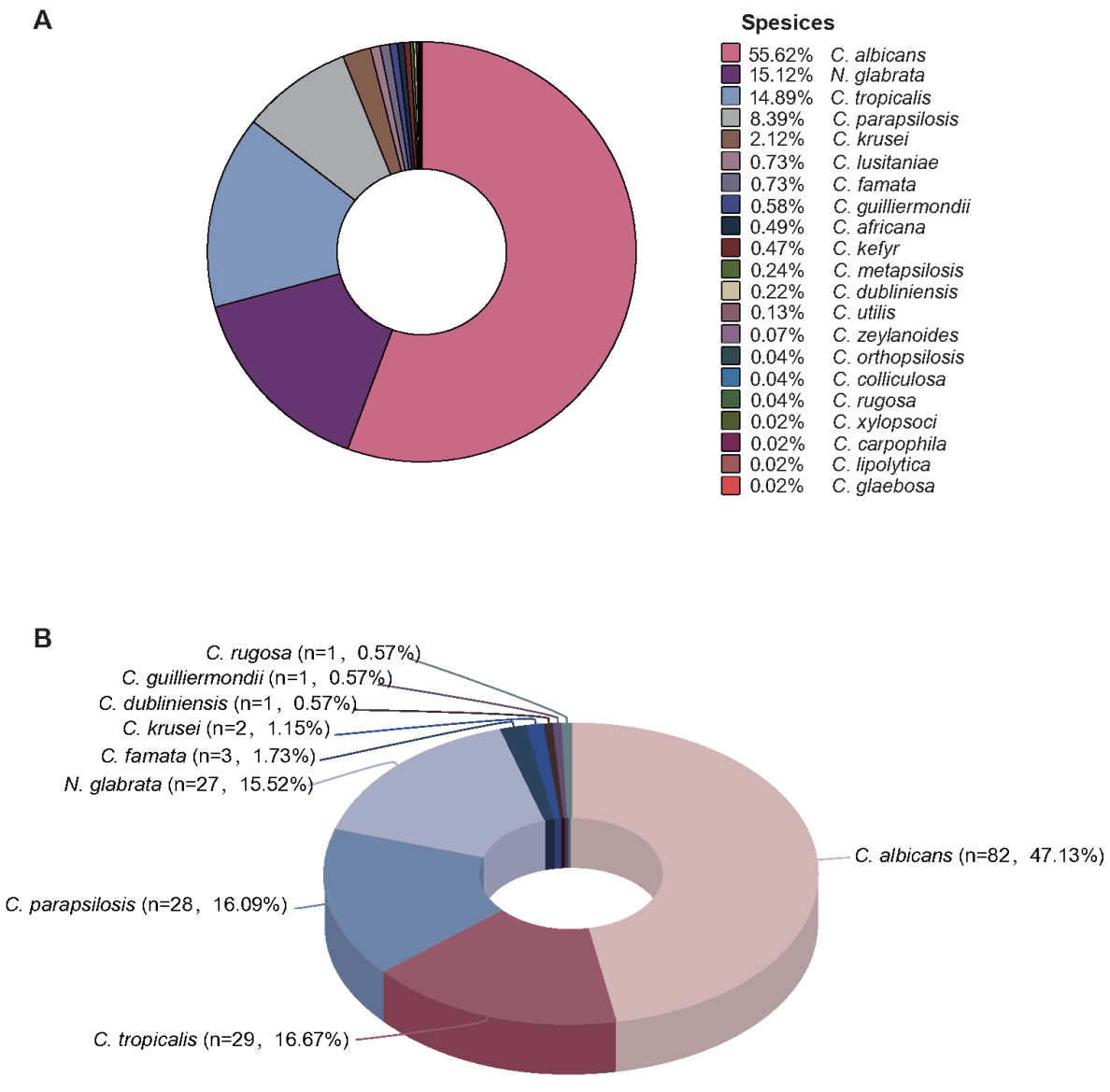

Figure 1 – Distribution of *Candida* proportions. (A) Prevalence of *Candida* in the overall patient cohort during the study. (B) Prevalence of *Candida* in patients with bloodstream infections throughout the study duration.

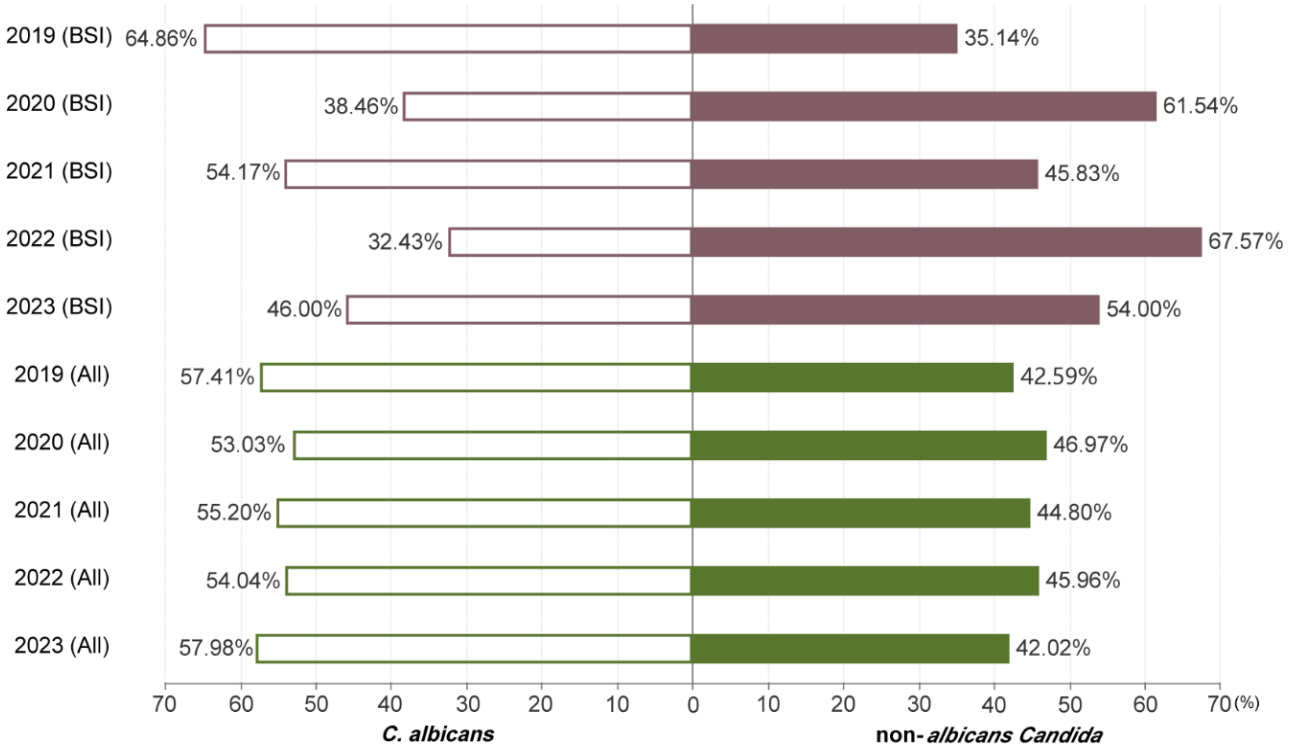

Figure 2 – Annual distribution of *C. albicans* versus non-*albicans Candida* infections. A two-way bar chart visually delineated the disparities between the two groups. "All" and "BSI" denoted distributions among all patients with *Candida* infections and, specifically, those with bloodstream infections over various years.

The age distribution of patients diagnosed with *Candida* infections was predominantly skewed towards older age groups, followed by young adulthood and middle adulthood categories (Fig. 3). Only six cases were reported in children. The median age of patients with *Candida* infections was 70 years (interquartile range [54–79]), with ages ranging from 1 day to 99 years (Fig. 3A). The age distribution of BSI patients also primarily favors older demographic, with young adult and middle adult groups trailing. Notably, there were no reported BSI cases in individuals younger than 18 years. The ages of BSI patients ranged from 31 to 94 years, with a median age of 70 years and an interquartile range of 55 to 78 years (Fig. 3B).

The ICU had the highest incidence of *Candida* infection cases, significantly outpacing that of obstetrics and gynecology, pulmonology, and urology (Fig. 4A). In contrast, most BSI cases were concentrated in the ICU, with only sporadic cases in other departments (Fig. 4B). This study assessed samples from 16 different sources to determine the proportion of *Candida* isolates. Sputum and urine contained the highest proportions of *Candida* isolates, followed by vaginal and general secretions following (Fig. 5). These results were consistent with the prevalence of common clinical samples in departments with a high concentration of *Candida* cases, such as the ICU, obstetrics and gynecology, pulmonology and urology.

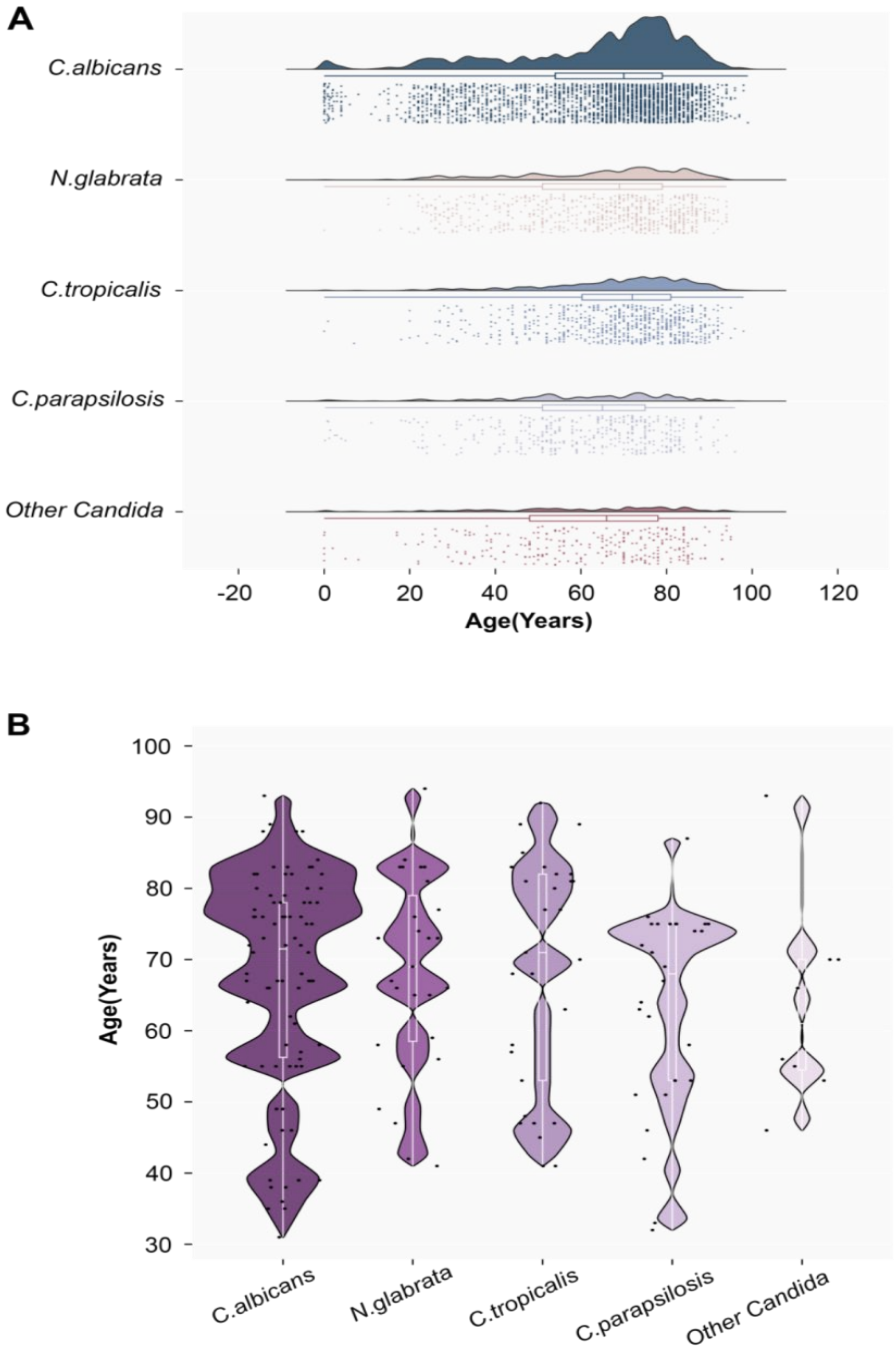

Figure 3 – Age distribution of *Candida* species. (A) Age distribution among patients with *Candida* Infections. The box plot nested in the violin plot depicts the interquartile range and the median, where the extent signifies the age range. The dimension of the cloud and the concentration of raindrops reflected the patient count per age group. Furthermore, "Other *Candida*" included species such as *C. utilis* (n=6), *C. dubliniensis* (n=10), *C. lipolytica* (n=1), *C. glaebosa* (n=1), *C. colliculosa* (n=2), *C. rugosa* (n=2), *C. carpophila* (n=1), *C. metapsilosis* (n=11), *C. orthopsilosis* (n=2), *C. xylopsoci* (n=1), and *C. zeylanoides* (n=3), mirroring its application in Fig. 4A, Fig. 5, and Table 1. (B) Age distribution of patients diagnosed with *Candida* BSI during the study period. The embedded box plot in the violin plot conveyed identical information to the box plot in the cloud diagram. The width of the violin plot represented the number of patients at a specific age. "Other *Candida*" included *C.*

krusei (n=2), *C. dubliniensis* (n=1), *C. guilliermondii* (n=1), *C. famata* (n=3), and *C. rugosa* (n=1). It was consistent with usage in Fig. 4B.

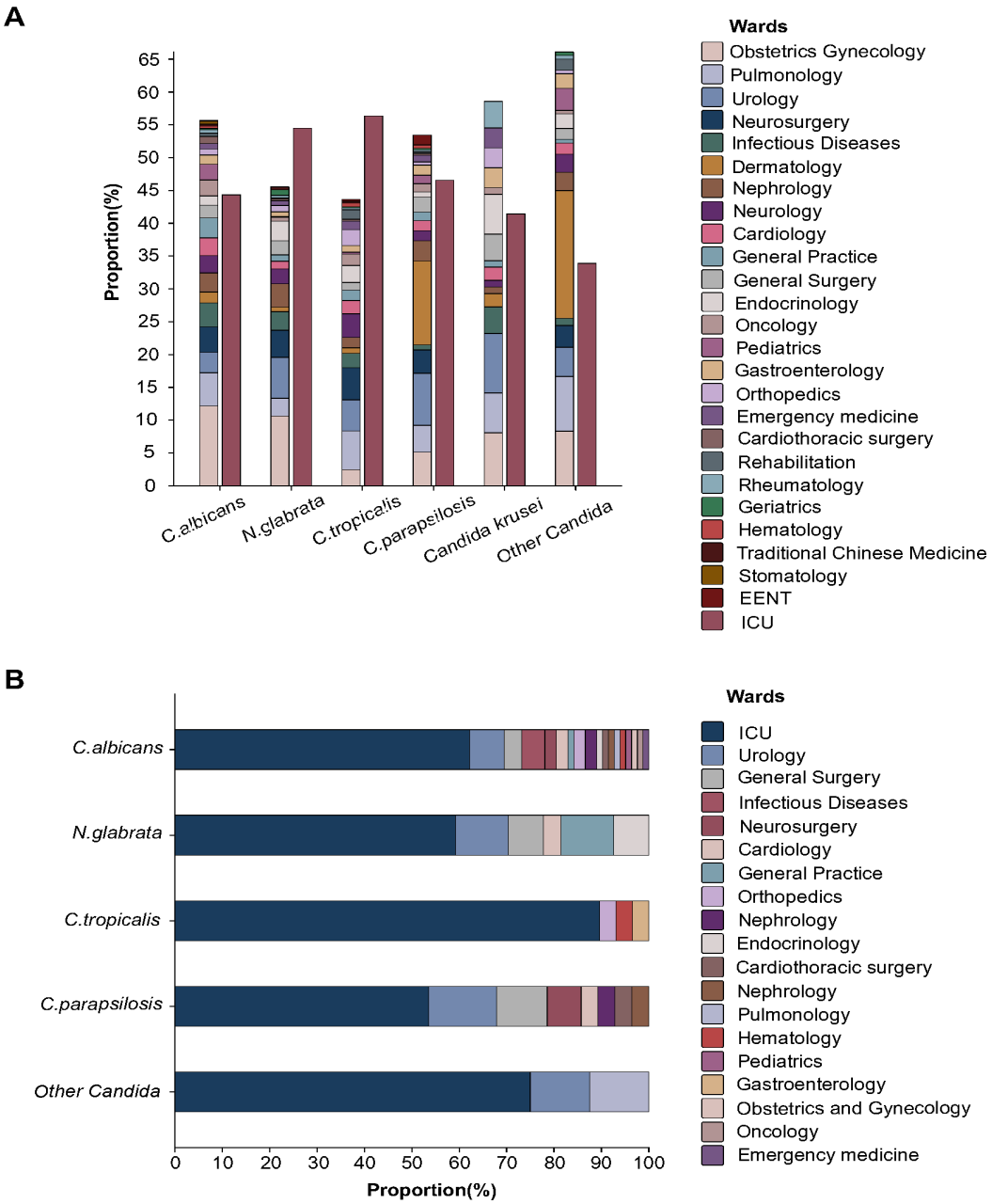

Figure 4 – Percentage distribution of *Candida* species across various hospital departments. (A) Proportional distribution of *Candida* species among departments for all patients with detected *Candida* infections during the study period. (B) Proportional distribution of *Candida* species among departments for patients with detected *Candida* BSI detected during the study period.

An overview of the clinical characteristics of patients infected with *Candida* was summarized (Table 1). Significant disparities were observed between *C. albicans* and NAC infections across different age groups. Additionally, male patients had a higher infection rate than females, with this trend being particularly notable for *C. tropicalis*, *C. famata*, *C. lusitaniae*, and *C. guilliermondii*, were particularly noticeable. For patients with BSI, males account for a higher proportion in cases

involving *C. tropicalis*, *C. parapsilosis*, and *C. famata*. Univariate analysis of comorbidities showed that most patients with *Candida* infections had at least one underlying health condition. Patients infected with *C. albicans* had significantly higher rates of ICU stays, respiratory dysfunction, and solid tumors, compared to those infected with NAC species, who had a higher prevalence of neurological diseases (predominantly in *C. tropicalis*, *C. parapsilosis*, and *N. glabrata*). In the BSI cohort, patients with NAC infections had a significantly higher prevalence of comorbid gastrointestinal pathology comorbidity than those with *C. albicans*, *C. tropicalis*, *C. parapsilosis*, *N. glabrata*, and *C. krusei* according for the majority of such cases.

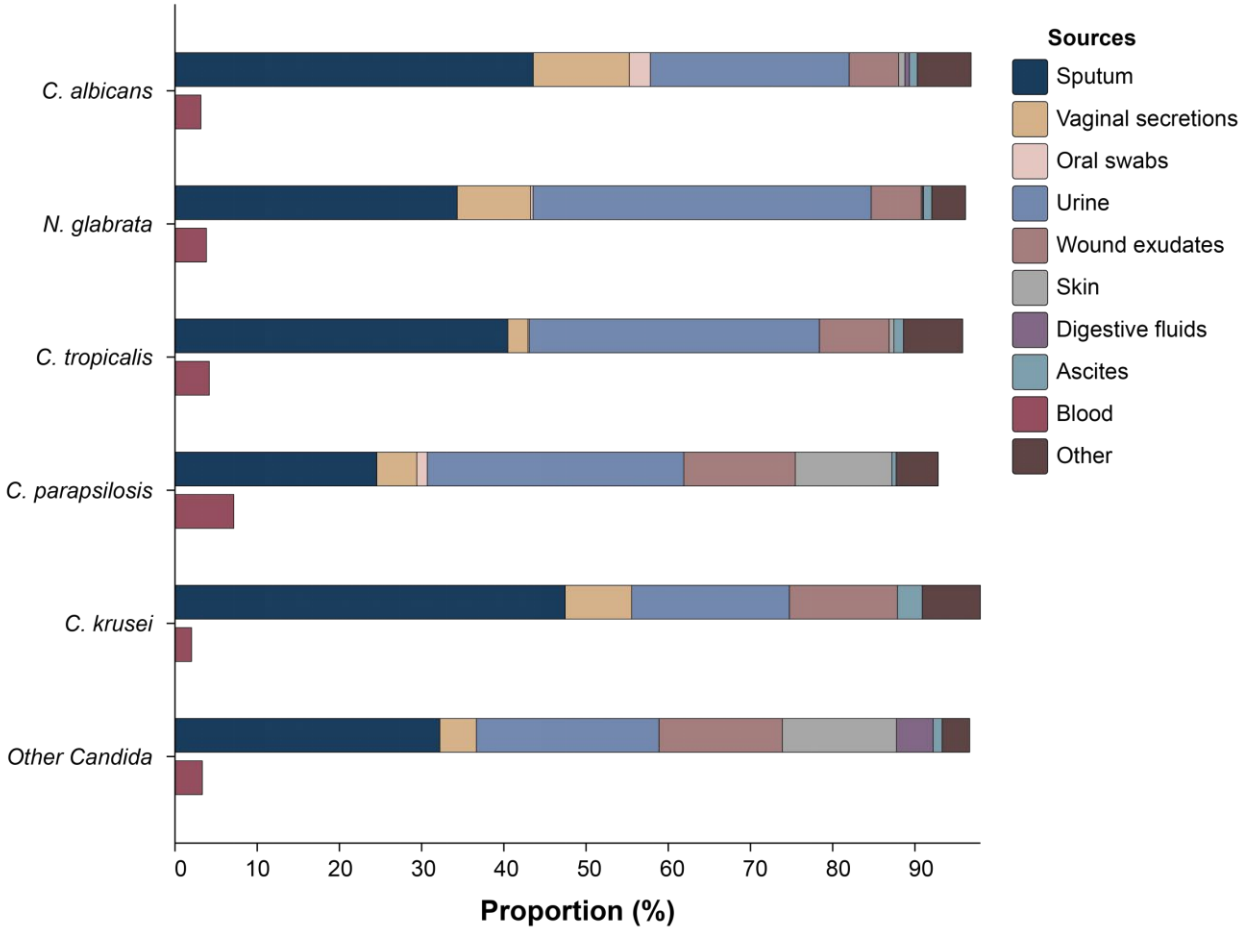

Figure 5 – Proportion of *Candida* species isolated from diverse sample sources. "Other" included samples from bronchoalveolar lavage fluid, bronchial brushing, effusion, stool, catheter tip, and cerebrospinal fluid.

Risk factors for *C. albicans* BSI compared with NAC bloodstream infection (Fig. 6, Table 2)

The binary logistic regression analysis evaluated the following independent variables to identify their association with candidemia caused by *C. albicans* or NAC species, including age, central venous catheter (CVC), catheters, mechanical ventilation, parenteral nutrition, surgery, ICU stay, application of antimicrobials, and receipt of corticosteroids in the context of candidemia due to *C. albicans* and NAC (Table 2). Forest plots were generated using R v4.3.1 (with the forest plot package) to visualize adjusted odds ratio (OR) and 95% confidence intervals derived from the final logistic regression model (Fig. 6). Analysis indicated that CVC utilization in NAC infections was associated with a higher odds ratio (OR 2.488; 95% CI 1.043-5.934) in contrast to *C. albicans* (OR

0.402; 95% CI 0.169-1.622). However, no statistically significant disparities were observed in the odds ratios for other aspects between candidemia caused by *C. albicans* and NAC, as clearly depicted in the forest plot clearly delineates ($P>0.05$).

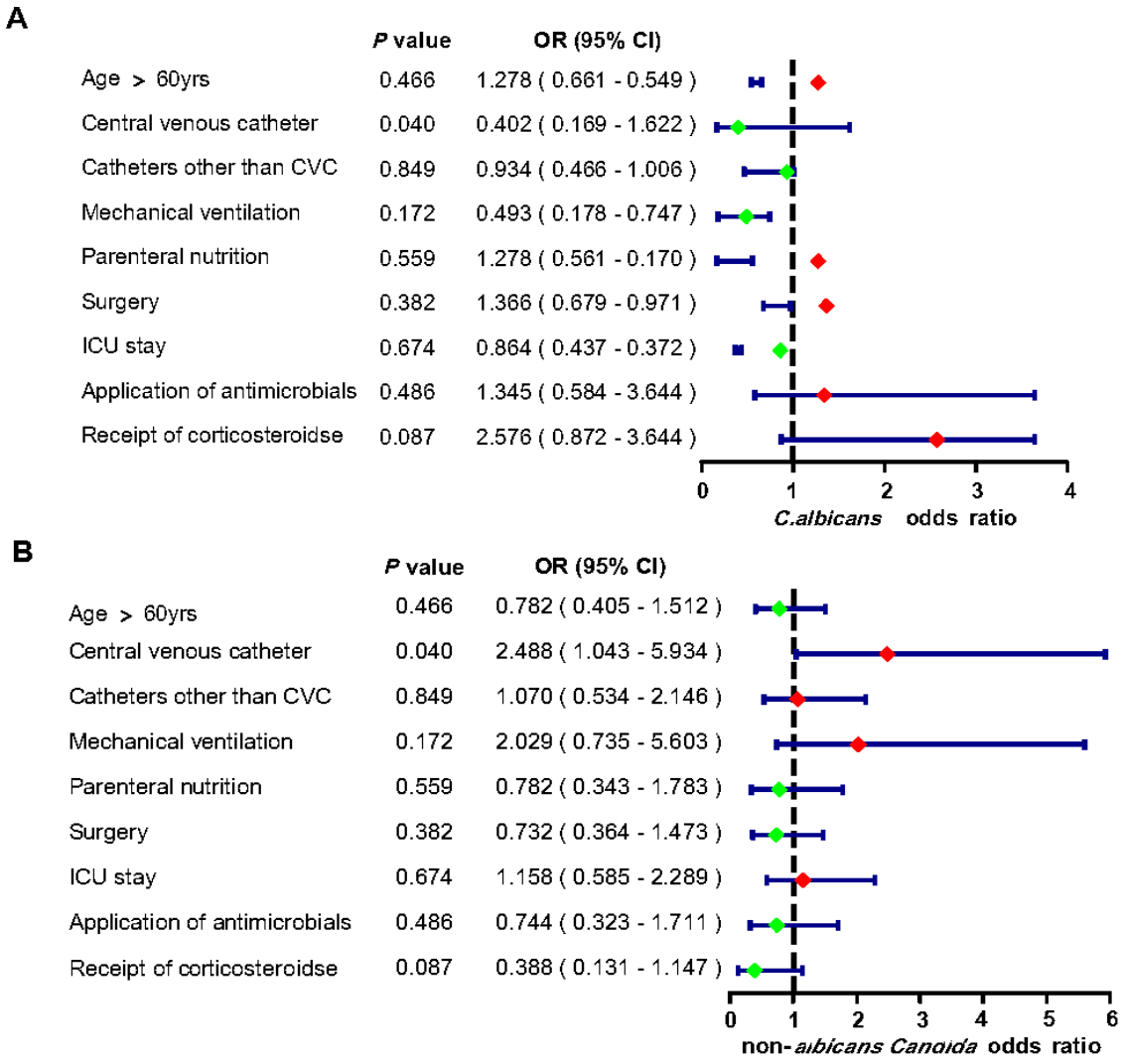

Figure 6 – Forest plot of risk factors associated with candidemia caused by *C. albicans* and non-*albicans Candida*. Stratified multivariable regression outputs: (A) visualizes adjusted odds ratios for predictors of *C. albicans* candidemia, while (B) displays risk estimates for non-*albicans Candida*. Horizontal bars represent 95% confidence intervals (CIs); diamond markers denote the overall effect size. The vertical line at OR = 1 indicates no effect.

Characterization of virulence traits in clinical *Candida* isolates: An *in vitro* assessment (Fig. 7) This study further identified the virulence characteristics of different strains by detecting the hyphal formation ability, biofilm formation ability, and extracellular protease secretion ability of clinical *Candida* isolates. *C. albicans* isolates from various clinical sources, together with non-*albicans Candida* isolates, were assessed for hyphal development in Spider medium (5×10^5 CFU/mL, 37 °C, 100 rpm, 4 h). Hyphal cells were quantified as the number of hyphae-forming cells per 100 yeast cells (Fig. 7A). Biofilm formation was measured via XTT staining after 24 h of incubation in RPMI-1640 (Fig. 7B).

Table 1 – Demographic and clinical data for patients with *Candida* infection.

Patient characteristics	All patients				Bloodstream infection patients			
	Total (n[%])	*C. albicans* (n[%])	NAC(n[%])	*P* value	Total (n[%])	*C. albicans* (n[%])	NAC (n[%])	*P* value
	(4662,100.00%)	(2593,55.62%)	(2069,44.38%)		(174,100.00%)	(82,47.13%)	(92,52.87%)	
Male	2531 (54.29)	1349 (52.02)	1182 (57.13)	0.001*	109 (62.64)	47 (57.32)	62 (67.39)	0.170
female	2131 (45.71)	1244 (47.98)	887 (42.87)		65 (37.36)	35 (42.68)	30 (32.61)	
Male: female	1.19: 1	1.08: 1	1.33: 1		1.68: 1	1.34: 1	2.07: 1	
Respiratory dysfunction	1075 (23.06)	685 (26.42)	390 (18.85)	<0.001*	24 (13.79)	14 (17.07)	10 (10.87)	0.236
Liver disease	34 (0.73)	22 (0.85)	12 (0.58)	0.285	5 (2.87)	1 (1.22)	4 (4.35)	0.436
CVD	158 (3.39)	84 (3.24)	74 (3.58)	0.527	6 (3.45)	4 (4.88)	2 (2.17)	0.576
Neurological disorders	826 (17.72)	390 (15.04)	436 (21.07)	<0.001*	16 (9.20)	8 (9.76)	8 (8.70)	0.809
Gastrointestinal pathology	275 (5.90)	142 (5.48)	133 (6.43)	0.170	11 (6.32)	1 (1.22)	10 (10.87)	0.011*
Renal failure	148 (3.17)	71 (2.74)	77 (3.72)	0.057	8 (4.60)	5 (6.10)	3 (3.26)	0.597
UTI	545 (11.69)	293 (11.30)	252 (12.18)	0.353	17 (9.77)	11 (13.41)	6 (6.52)	0.126
Solid tumor	245 (5.26)	168 (6.48)	77 (3.72)	<0.001*	20 (11.49)	10 (12.20)	10 (10.87)	0.784
Hematological malignancy	60 (1.29)	32 (1.23)	28 (1.35)	0.720	5 (2.87)	3 (3.66)	2 (2.17)	0.896
Bone diseases	167 (3.58)	88 (3.39)	79 (3.82)	0.438	18 (10.34)	10 (12.20)	8 (8.70)	0.449
Compromised skin	85 (1.82)	39 (1.50)	46 (2.22)	0.068	0 (0.00)	0 (0.00)	0 (0.00)	-
Diabetes mellitus	159 (3.41)	78 (3.01)	81 (3.91)	0.090	9 (5.17)	4 (4.88)	5 (5.43)	1.000
Hypertension	44 (0.94)	27 (1.04)	17 (0.82)	0.441	1 (0.57)	0 (0.00)	1 (1.09)	1.000
Pregnancy	100 (2.15)	57 (2.20)	43 (2.08)	0.779	0 (0.00)	0 (0.00)	0 (0.00)	-

Patient characteristics	All patients				Bloodstream infection patients			
	Total (n[%])	*C. albicans* (n[%])	NAC(n[%])	*P* value	Total (n[%])	*C. albicans* (n[%])	NAC (n[%])	*P* value
	(4662,100.00%)	(2593,55.62%)	(2069,44.38%)		(174,100.00%)	(82,47.13%)	(92,52.87%)	
Fever (T>38℃)	150 (3.22)	74 (2.85)	76 (3.67)	0.115	7 (4.02)	3 (3.66)	4 (4.35)	1.000

***** *P* was statistically significant. CVD: Cardiovascular disease, UTI: Urinary tract infection, NAC: non-*albicans Candida.*

Table 2 – Odd ratios of risk factors associated with candidemia caused by *Candida albicans* and non-*albicans Candida.*

Variables	*C. albicans*			non-*albicans Candida*			*P* value
	OR*	95% Cl*		OR	95% Cl		
		Lower	Upper		Lower	Upper	
Age ＞ 60yrs	1.278	0.661	0.5493	0.782	0.405	1.512	0.466
Central venous catheter	0.402	0.169	1.6222	2.488	1.043	5.934	0.040*
Catheters other than CVC	0.934	0.466	1.0064	1.070	0.534	2.146	0.849
Mechanical ventilation	0.493	0.178	0.7465	2.029	0.735	5.603	0.172
Parenteral nutrition	1.278	0.561	0.1699	0.782	0.343	1.783	0.559
Surgery	1.366	0.679	0.9709	0.732	0.364	1.473	0.382
ICU stay	0.864	0.437	0.3721	1.158	0.585	2.289	0.674
Application of antimicrobials	1.345	0.584	3.6441	0.744	0.323	1.711	0.486
Receipt of corticosteroids	2.576	0.872	3.6441	0.388	0.131	1.147	0.087

***** *P* was statistically significant; OR = odds ratio. The metric was used to calculate the ratio of two rates, evaluating the strength of association between a specific exposure and a given disease; CI: confidence interval, CVC: Central venous catheter, ICU: Intensive Care Unit.

Protease and phospholipase activities were evaluated using egg yolk and bovine serum albumin media (Fig. 7C,7D). The results showed that blood-derived *C. albicans* isolates exhibited the strongest virulence triad: the proportion of hyphal cells was 80.4 ± 3.49%, biofilm biomass reached 0.1213 ± 0.0107, proteinase (SAP) activity was 0.356 ± 0.057 (high activity), and phospholipase PL activity was 0.564 ± 0.036 (medium activity). Notably, mucosal-derived strains (oral/vaginal) also presented a high virulence phenotype, with hyphal formation rates (74.6 ± 3.97%, 72.40 ± 4.04%), biofilm levels (0.1094 ± 0.0158, 0.106 ± 0.014), and proteinase activities (0.444 ± 0.07, 0.45 ± 0.059) approaching those of blood-derived isolates. In contrast, *C. albicans* isolates from urine, skin, and digestive fluids showed weaker hyphal and biofilm formation abilities, as well as lower extracellular protease secretion.

Among non-*albicans Candida* strains, the virulence of *C. tropicalis* was comparable to that of highly invasive *C. albicans* strains: the hyphal formation rate was 65.6 ± 5.32%, the OD_{490} value of the biofilm was 0.0998 ± 0.0051 (second only to the mucosal-derived strains), and the proteinase and phospholipase activities (0.502 ± 0.04 and 0.45 ± 0.059, respectively) were significantly stronger than those of other non-*albicans Candida* strains ($P < 0.01$). The non-hyphal-forming *N. glabrata* exhibited a unique pattern: it lacked hyphal formation ability, formed biofilms through yeast aggregates (0.0844 ± 0.007), and showed no protease activity (Pz > 0.9). *C. krusei* was less virulent than the weakly hyphal-forming *C. parapsilosis*: the former relied on phospholipase (0.582 ± 0.038) rather than proteinase (0.862 ± 0.029), while the latter had weak biofilm formation ability (0.0464 ± 0.0077) but relatively strong hyphal activity (41.4 ± 4.98%).

***In vivo* assessment of virulence in *Candida albicans* from varied clinical samples** (Fig. 8)

Eighteen *C. albicans* strains, originating from nine distinct sample types (sputum, vaginal secretions, oral swabs, urine, wound exudates, skin, blood, digestive fluids, and ascites), were selected to assess virulence in mice. Additionally, virulence was quantitatively evaluated for all 65 clinical isolates using the *Galleria mellonella* infection model. Substantial differences in mortality rates were observed within 10 days post-infection in both the *Galleria mellonella* and mouse models. Median survival durations ranged from 4 to 5 days for *Galleria mellonella* and 3 to 6.5 days for the mouse model (Fig. S1, Fig. 8A). Mortality was most pronounced in the groups infected with blood-derived strains. This result was also reflected in pathological examination of mouse kidneys: blood-derived strains caused severe renal damage and triggered a significant inflammatory response (Fig. S2). The PBS control group showed no fatalities (Fig. 8A). Fungal burden analysis revealed a notably higher fungal burden load in blood-derived strains (Fig. 8B). Virulence test results were consistent across both *in vivo* models, with blood-sourced strains exhibiting the strongest virulence.

The inflammatory cytokine response induced in mice following *Candida albicans* Infection (Fig. 9)

ELISA analysis of serum from mice infected with *C. albicans* revealed increased levels of IL-2, IL-4, IL-10, and IL-17A cytokines in all infected groups compared to the PBS control group. As showed in Fig.9, IL-2 and IL-17A levels were lowest in the group with blood-derived infections group but higher in groups infected with strains derived from sputum and wound secretions. In contrast, IL-4 and IL-10 levels were highest in the blood-derived infections group and lower in groups infected with strains from sputum, oral swabs, and wound secretions. No significant differences in cytokine levels were observed between groups infected with strains from vaginal secretions, digestive fluids, or ascites and other groups. These findings indicated that local adaptive immunity, involving Th1, Th2, and Th17 responses, played a significant role in the host's immune defense against *C. albicans* infection.

DISCUSSION

Candida, a widespread pathogen causing invasive mycosis in humans, primarily manifests as both superficial and deep infections (Lu et al. 2023). Among these infections, candidemia,

characterized by *Candida* bloodstream infections, is regarded as the most severe form (Lass-Flörl et al. 2024). Our findings show a consistent increase in the incidence of both candidiasis and *Candida* BSIs over the past five years, which aligns with previous studies but contrasts with plateauing trends reported in East China (Pfaller et al. 2020, Ulu Kilic et al. 2017). Notably, the proportion of *Candida* infections was lowest in 2020 and 2021. China's approach to managing the COVID-19 epidemic likely constrained the identification and documentation of non-severe *Candida* cases, in stark contrast to global surges: U.S. hospitals reported 31% increase in candidemia during pandemic peaks, driven by immunoparalysis and corticosteroid therapies (Seagle et al. 2022). *C. albicans* remains more prevalent than NAC, consistent with observations in other regions of China (Hou et al. 2022, Pappas et al. 2018). However, a global rise in common NAC species has been documented, and in our study, NAC strains account for over half of *Candida* BSIs (Bilal et al. 2023, Pu et al. 2017). Among NAC infections, *N. glabrata* is the most common overall, while *C. tropicalis* predominates in *Candida* BSIs, a pattern consistent with other studies (Verma et al. 2021, Ngamchokwathana et al. 2021). However, China exhibits striking geographical disparities: Eastern provinces-maintained *C. albicans* dominance, while Northern regions reported surges in *C. parapsilosis* (Hong et al. 2022, Zhang et al. 2021). Our Southwestern cohort showed an unparalleled prevalence of *C. tropicalis* (32.6% of BSIs; Fig. 1B). The significant predominance of NAC (>50% of BSIs) mirrors epidemiological shifts in industrialized nations like Germany yet exceeds rates documented in North China (Xiao et al. 2018). The observed parallels with tropical regions (where *C. tropicalis* is endemic) and divergence from temperate zones (dominated by *N. glabrata*) suggest climate-mediated pathogen adaptation.

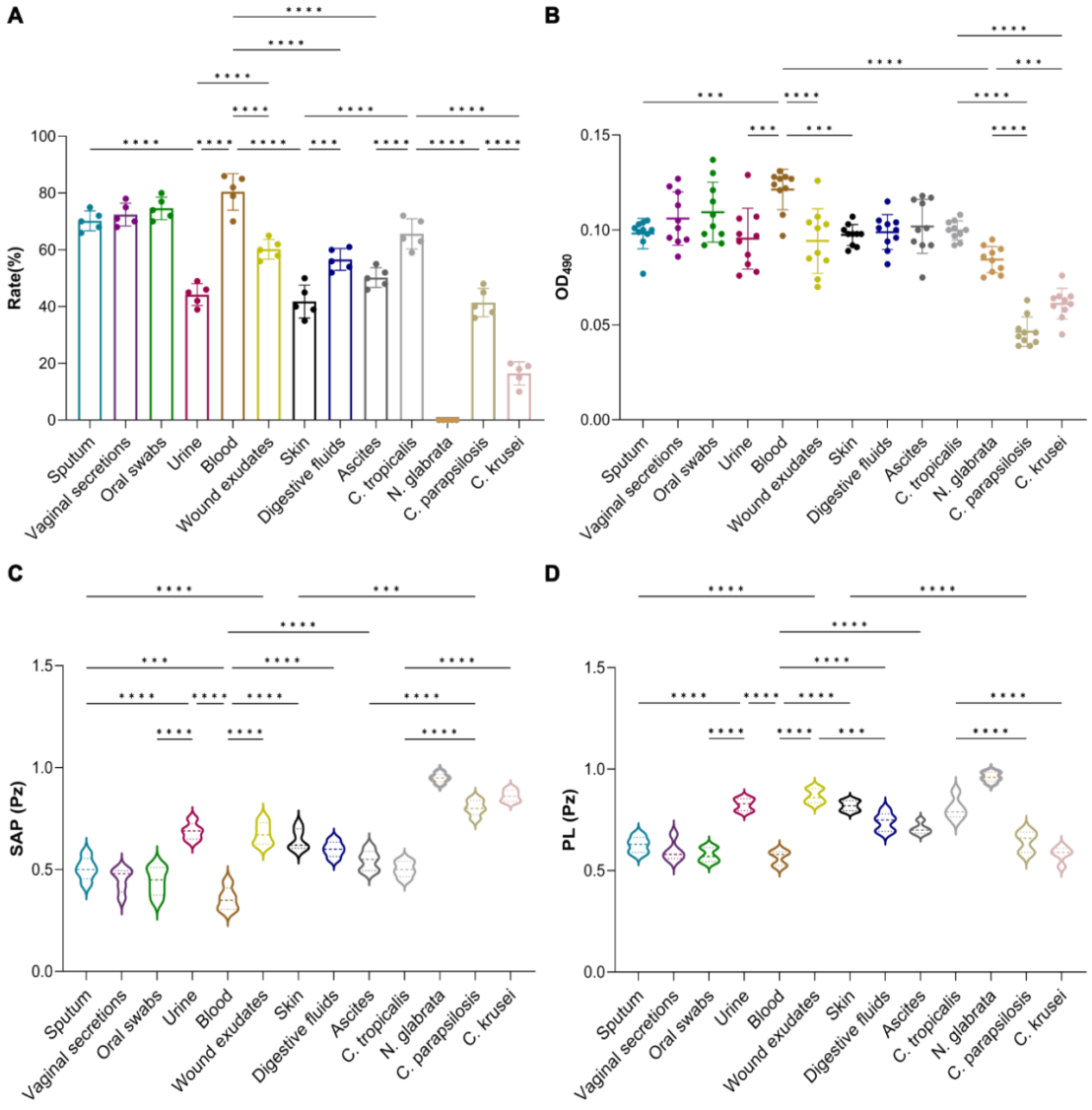

Figure 7 – Analysis of the virulence phenotypes of clinical *Candida* isolates. (A) Hyphal formation rates among different isolates. (B) Biofilm biomass (OD_{490}). (C, D) Hydrolytic enzyme activities (SAP and PL). Each experimental procedure was replicated at least 2-3 times. Data presented as mean ± SD, ANOVA with Tukey's multiple comparisons (GraphPad Prism 9.0). $^{*}P < 0.0332$, $^{**}P < 0.0021$, $^{***}P < 0.0002$, $^{****}P < 0.0001$.

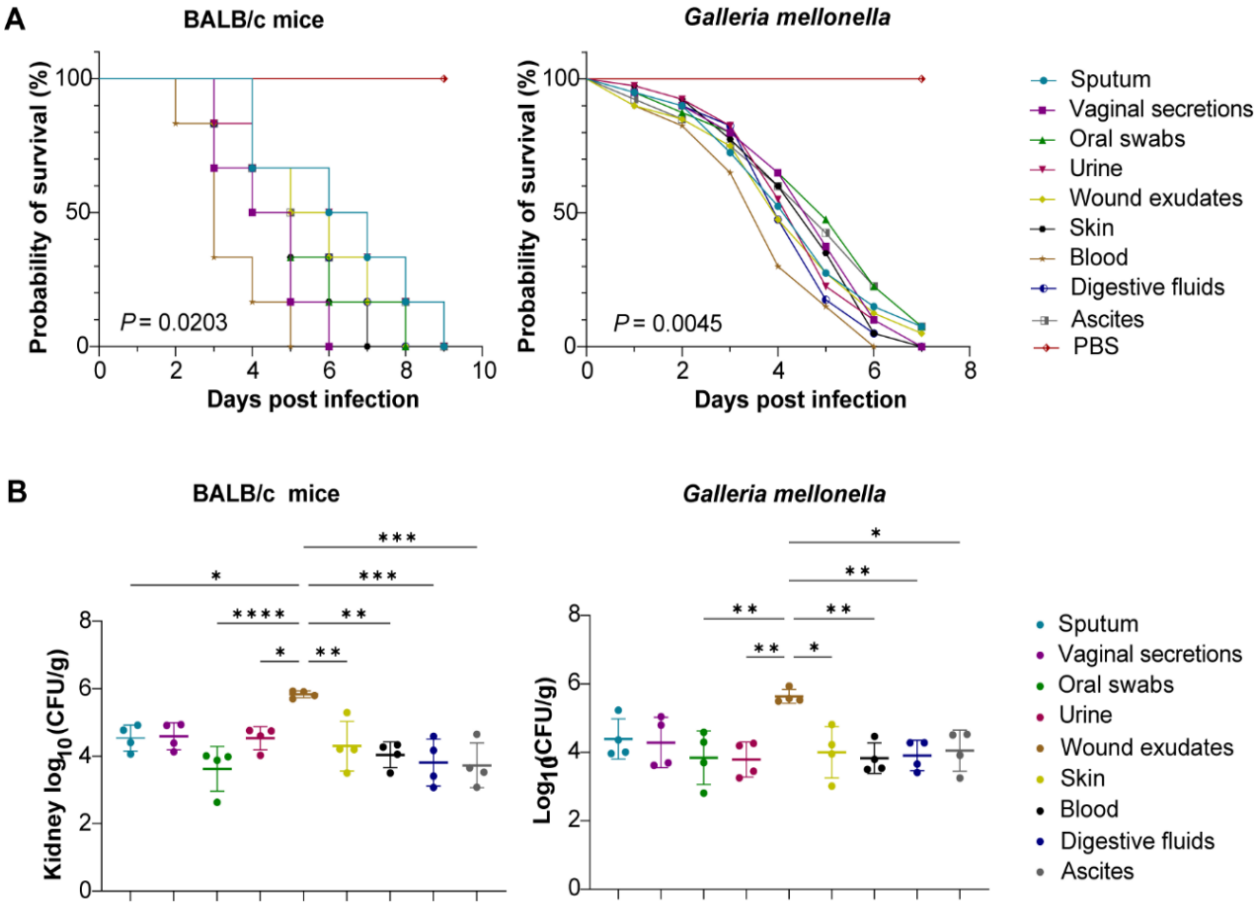

Figure 8 – The survival rates and tissue fungal burdens in *Galleria mellonella* and BALB/c mice after infection with *C. albicans* strains of different origins. (A) Both *Galleria mellonella* larvae and mice were inoculated with a *C. albicans* suspension at a concentration of 2×10^5 CFU/mL. Mortality was monitored at fixed intervals, and Kaplan-Meier survival curves were used to illustrate the survival dynamics. (B) On day 3 post-infection, both larvae and mice were humanely euthanized. Tissue samples from the larvae and kidneys of the mice were weighed, homogenized, appropriately diluted, and then plated on SDA to assess fungal burden. Each experimental procedure was replicated at least 2-3 times, with data presented as mean ± SD. One-way ANOVA was conducted to analyze the data. $^{*}P < 0.0332$, $^{**}P < 0.0021$, $^{***}P < 0.0002$, $^{****}P < 0.0001$.

Candida infections are concentrated among adults and the elderly, with infection rates rising with age. This reflects increased susceptibility to *Candida* in older individuals due to impaired immune function, damaged mucosal barriers, and underlying severe diseases (BourassaBlanchette et al. 2023). Newborns, particularly preterm infants, were also at high risk of *Candida* infections. Most of these newborns are in the ICU, and their immature immune systems and underdeveloped epithelial barriers make them vulnerable to such infections (Shuping et al. 2021). Surprisingly, the absence of pediatric BSI cases distinguishes our cohort from North American surveillance, where children account for 10-20% of candidemia cases (Benedict et al. 2023). This discrepancy warrants investigation into regional neonatal antifungal prophylaxis protocols. The ICU has the highest

epidemiological prominence, accounting for 47.1% of cases, exceeding rates in Central China but comparable to Brazilian ICUs, where candidemia prevalence reaches 50% (Sieben et al. 2023). However, the secondary prominence of obstetrics/gynecology departments (19.3%) is a uniquely Asian phenomenon, aligning with studies from China that attribute 28% of vulvovaginal candidiasis to healthcare exposure (Ge et al. 2022). The ICU had the highest infection rate among hospital departments, followed by the obstetrics and gynecology department. The high incidence of *Candida* infections in the obstetrics and gynecology department can be partially attributed to recurrent vulvovaginal candidiasis (Lietz et al. 2023, Weimer et al. 2021). This study found a higher incidence of *Candida* infections in males than in females. The male predominance (62.1%) is consistent with reports from Southeast Asian but contrasts with gender-neutral distribution in European cohorts (Arendrup et al. 2023). Gender differences in candidiasis prevalence may be influenced by biological factors such as sex hormones and gender-specific immune responses (Jenks et al. 2023). These findings place Southwest China within a global epidemiological transition marked by the rise of NAC and increased susceptibility among the elderly.

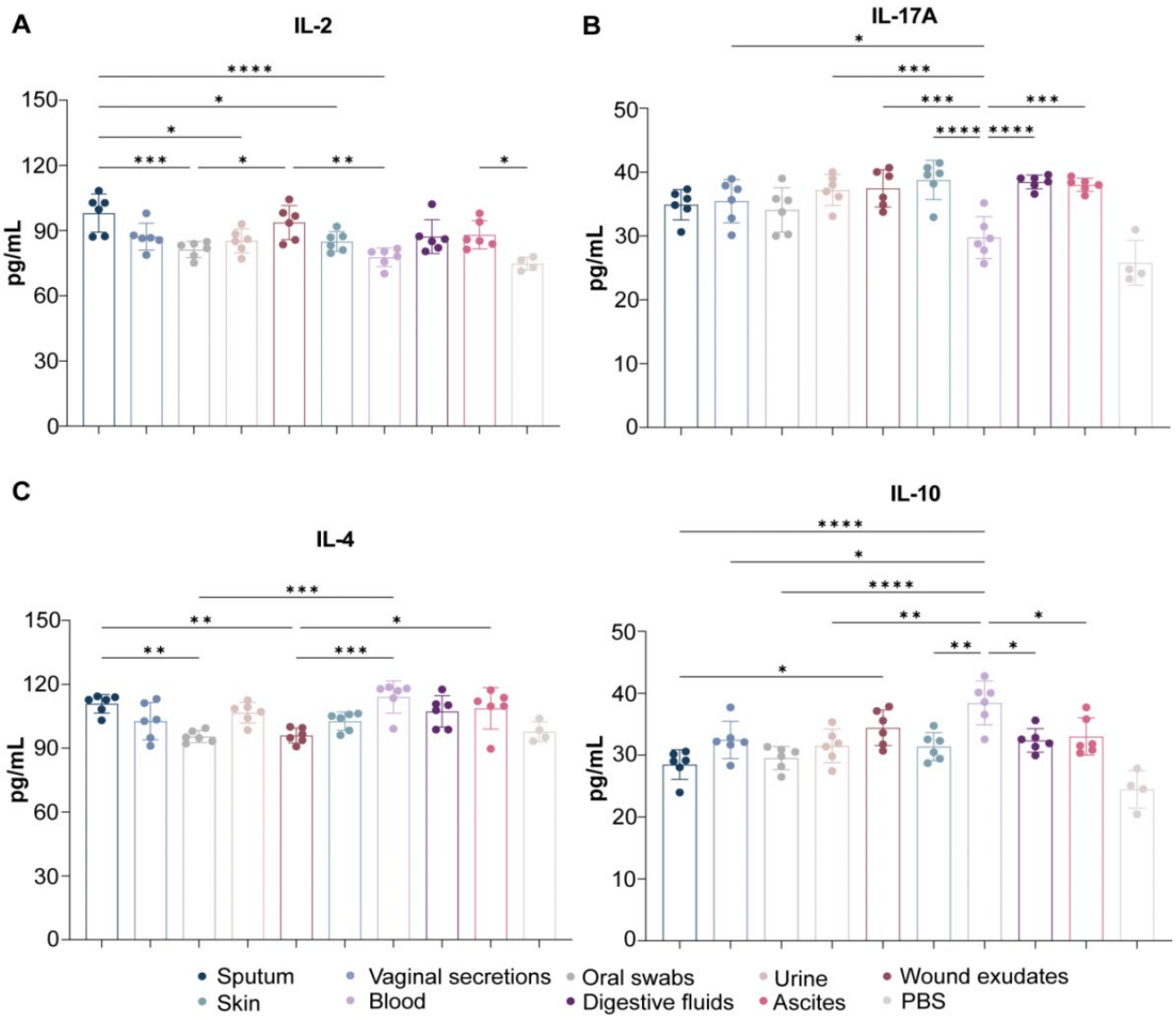

Figure 9 – The changes in serum cytokine levels among mice from different infection groups. After infection with *C. albicans* strains of various origins, serum samples were collected from each group of BALB/c mice, and cytokine concentrations were measured using ELISA. The serum levels of IL-2 (A), IL-17A (B), IL-4 and IL-10 (C) cytokines related to Th1, Th17 and Th2 cell responses were assessed. Each experimental assay was repeated at least 2-3 times, with data reported as mean ± SD. $^{*}P < 0.0332$, $^{**}P < 0.0021$, $^{***}P < 0.0002$, $^{****}P < 0.0001$.

Most patients with *Candida* infection in this study had at least one comorbidity, particularly ICU admission, respiratory dysfunction, solid tumors, and neurological disorders. In cases of *Candida* BSIs, NAC showed a higher prevalence of comorbid gastrointestinal pathology compared to *C. albicans*. The observed association between NAC BSIs and gastrointestinal comorbidities in our study aligns with American data (Simon et al. 2021), suggesting shared pathogenic mechanisms across Asian populations. However, the predominant link between gastrointestinal pathology and NAC-BSI in our cohort differs significantly from reports in Central China. This divergence may result from regional variations in three aspects: (1) Antibiotic stewardship: The use of broad-spectrum cephalosporin in ICUs of Southwest China (62 DDD/1000 patient-days) exceeds WHO recommendations. (2) Microbiota profiles: The preference of Bacteroides in patients from Southwest China is 75%, compared to 53% in coastal regions. (3) Dietary factors: Spicy cuisine may potentially exacerbate the compromise of mucosal integrity. Conditions such as extensive full-thickness burns, gastrointestinal perforation, and acute or necrotizing pancreatitis can disrupt the skin or mucosal barrier, promoting the proliferation of *Candida* and its potential dissemination into the bloodstream (Hoenigl et al. 2023). Multivariate logistic regression analysis indicated that the presence of CVC is an independent risk factor for *Candida* BSI. The differential risk of CVC for NAC-BSI in our study is consistent with data from Brazilian ICUs (Sieben et al. 2023). However, it contrasts with findings from European ICUs, where CVC-associated NAC-BSI rates are uniform across species, and US data identifying peripherally inserted central catheters (PICCs) as the primary risk factor (Arendrup et al. 2023, Seagle et al. 2022). The non-significant association with mechanical ventilation (MV) in our study represents a major deviation from global consensus, which may be explained by shorter MV duration in Southwest China (median 4.2 d vs 8.7 d globally) and higher early extubating rates (62% within 48h vs. 38% in EPIC II study). Patients requiring long-term intravenous infusions or using indwelling prosthetic materials are at an increased risk of invasive disease due to compromised anatomical defenses and colonization of hand skin flora (Ricotta et al. 2020).

The virulence of *C. albicans* varies depending on factors such as species variation, geographical disparities, host immune responses, and the progression of infection (Rottmann et al. 2020). The use of animal models to assess the virulence of *Candida* strains provides an additional pathway to deepen our understanding of the cumulative effects of virulence determinants on patient outcomes (Mroczyńska et al. 2021). This study showed that the virulence of *C. albicans* is strongly dependent on the tissue source. Bloodstream isolates exhibited a complete virulence triad (hyphal formation: 80.4% ± 3.49%; biofilm: OD_{490} 0.1213 ± 0.0107; SAP/PL activity: 0.356/0.564) and caused rapid lethality (median survival: 78 h in *G. mellonella*, 3 days in mice), extensive histopathological changes (diffuse renal microabscesses with fibrinoid necrosis) and the highest fungal burden (2.3× renal load compared to other isolates). Mucosal isolates showed niche-specific adaptations, including near-bloodstream hyphal competence, elevated protease activity for epithelial penetration, and cortical-restricted renal damage, reflecting evolutionary trade-offs. *C. tropicalis* approached the virulence of bloodstream *C. albicans*, while *N. glabrata* relies on yeast aggregation without depending on protease, which is consistent with research in Brazil. These findings align with previous studies on the virulence of *Candida* strains from various clinical sources in South Africa and other regions (Marcos-Zambrano et al. 2020). Cytokine profiling of murine systemic *C. albicans* infection (Fig. 9) revealed distinct immune reprogramming patterns directly related to the isolation sources of the strains. Bloodstream-derived isolates induced elevated IL-4 and IL-10 expression, accompanied by suppressed IL-2 and IL-17A, indicating a dual immunological adaptation. This cytokine profile reflects Th2 skewing, which prioritizes humoral immunity over phagocyte-mediated clearance mechanisms, along with robust regulatory T cell (Treg) induction, where IL-10 actively inhibits dendritic cell maturation and suppresses Th1/Th17 differentiation (Liao et al. 2024, Break et al. 2021). Infections with sputum and wound-derived isolates showed significant elevation of IL-17A and IL-2, which is associated with specialized barrier defenses. IL-17A promotes neutrophil recruitment and enhances epithelial barrier integrity against fungal invasion, while the concurrent upregulation of IL-2 expands tissue-resident memory T cells (TRM) to establish localized protective immunity (Bose et al. 2024, Break et al. 2021). Evolutionarily, these strains adapt by utilizing tissue-specific

inflammation to optimize their persistence in mucosal niches. The minimal cytokine fluctuations observed in gut/ascites-derived infections reflect two synergistic adaptation strategies. Intrinsic TGF-β-mediated immunosuppression establishes local immune tolerance in gastrointestinal environments (Pappas et al. 2018). This discussion connects our cytokine data with principles of evolutionary immunology, providing actionable diagnostic and therapeutic insights specific to the ecological characteristics of *C. albicans* strains.

However, it is crucial to acknowledge several limitations of this study. First, clinical *Candida* isolates were identified using time-of-flight mass spectrometry, which carries a potential risk of bias in strain identification due to limitations within the strain library. Although experimental strains were re-identified via ITS molecular analysis, most were not subjected to sequencing. Additionally, this study is retrospective and restricted to a specific region, which may compromise variable control and introduce bias into the results. Factors such as regional population distribution, medical intervention levels, and patient type distribution could influence the data obtained. We explicitly recognize that while virulence phenotypes and cytokine responses (IL-2, IL-4, IL-10, IL-17A) observed in *Galleria mellonella* and BALB/c models provide comparative insights into strain behavior, immune-pathological profiles cannot be directly extrapolated to human candidemia. This is due to multifaceted clinical complexities, including iatrogenic immunosuppression, comorbidities (*e.g.*, diabetes, malignancies), microbiome dysbiosis, and healthcare-associated exposures during prolonged hospitalization (Casadevall et al. 2022). *Galleria mellonella* inherently lacks adaptive immunity and thus fails to recapitulate human-specific defenses: antigen presentation, Th17-polarized responses, FcγR-mediated fungal clearance, and neutrophil extracellular trap formation, mechanisms preserved only in vertebrate hosts (Tsai et al. 2016). Despite their abilities to model systemic infection, BALB/c mice exhibit marked differences from humans, including lower cytokine regulation thresholds (10-fold lower IL-17A activation), distinct immune cell activation kinetics (TLR4 hyperresponsiveness to β-glucans), and limited breadth in modeling immunosuppression (restricted to glucocorticoids versus multi-drug clinical regimens) (Casadevall et al. 2022). The elevated IL-17A levels correlating with renal fungal burden reflect murine-specific neutrophil recruitment pathways rather than clinical immunosuppressive states; such divergence stems from species-specific regulatory mechanisms, the γδ T cell-dominated rapid responses in mice versus $CD161^{+}$ MAIT cell-mediated regulation in humans (Gaffen et al. 2017). Notwithstanding these limitations, our dual-model system demonstrates clinical relevance: virulence stratification (bloodstream > mucosal > non-sterile isolates) prospectively identified treatment failures in matched ICU isolates, establishing a risk-stratification framework for high-risk strains warranting clinical prioritization (Liu et al. 2025). Future validation should incorporate humanized models with patient-derived immune cells and longitudinal cytokine monitoring in immunosuppressed cohorts.

This study analyzed clinical data from 4662 hospitalized patients in tertiary medical facilities in Southwest China over the past five years. The results showed that *C. albicans* is the predominant cause of *Candida* infections in this region. Among the identified risk factors, CVC use was recognized as a high-risk factor for non-*albicans Candida* BSI. Notably, the clinical origin of *Candida* strains critically impacts their pathobiological potential: bloodstream isolates exhibit the strongest expression of invasive virulence determinants, including robust hyphal formation, dense biofilm production, high protease activity, and strong pathogenicity. Correspondingly, the host's inflammatory cytokine responses induced after infection also vary with the strain source. Future research will focus on exploring the prevalence of candidiasis in underdeveloped regions, investigating epidemiological disparities across different areas, classifying isolates, and assessing patient prognosis. These efforts aim to develop region-specific strategies for the effective prevention and treatment of candidiasis.

ACKNOWLEDGEMENTS

This work was supported by the National Key R&D Program of China (2024YFC2309600; 2022YFC2303203); 111 Project (D20009); National Natural Science Foundation of China (32170195; 32060034; 32311530119; 32070146, 32200161); Major Science and Technology Plan

Project of China National Tobacco Corporation [110202101048 (LS-08)]; China–Ukraine Intergovernmental Exchange Project (8); Shanghai Science and Technology Innovation Action Plan 2023 “Basic Research Project”(23JC1404201); Guizhou High-level Innovative Talents Project (qiankeherencai-GCC[2022]036–1); Foundation of Key Laboratory of Microbiology and Parasitology of Education Department, Guizhou (QJJ [2022] 019); The Guizhou Province Science and Technology Plan project (Qiankehe Foundation - ZK [2023] general 332). We thank Professor Nalin N. Wijayawardene (Qujing Normal University) for language editing of the manuscript and scientific refinement of this manuscript.

CONFLICT OF INTEREST

The authors declare no conflicts of interest regarding this article.

REFERENCES

Arendrup MC, Arikan-Akdagli S, Jørgensen KM, Barac A et al. 2023 – European candidaemia is characterised by notable differential epidemiology and susceptibility pattern: Results from the ECMM *Candida* III study. Journal of Infection 87(5), 428–437.

Benedict K, Roy M, Kabbani S, Anderson EJ et al. 2018 – Neonatal and pediatric candidemia: Results from population-based active laboratory surveillance in four US locations, 2009-2015. Journal of the Pediatric Infectious Diseases Society (3), 3.

Bilal H, Zhang D, Shafiq M, Khan M et al. 2023 – Six-Year retrospective analysis of epidemiology, risk factors, and antifungal susceptibilities of candidiasis from a tertiary care hospital in South China. Microbiology spectrum 11(4), e0070823–e0070823.

BourassaBlanchette S, Biesheuvel M, Lam J, Kipp A et al. 2023 – Incidence, susceptibility and outcomes of candidemia in adults living in Calgary, Alberta, *Canada* (2010-2018). MC infectious diseases 23(1), 100.

Bose S, Sahu SR, Dutta A, Acharya N 2024 –A chemically induced attenuated strain of *Candida albicans* generates robust protective immune responses and prevents systemic candidiasis development. eLife 13, RP93760.

Break TJ, Oikonomou V, Dutzan N, Desai JV et al. 2021 – Aberrant type 1 immunity drives susceptibility to mucosal fungal infections. Science 371(6526), eaay5731.

Feng Z, Lu H, Jiang Y. 2024 – Promising immunotherapeutic targets for treating candidiasis. Frontiers in Cellular and Infection Microbiology 14, 1339501.

Frank D, Naseem S, Russo G, Li C et al. 2018 – Phagocytes from mice lacking the sts phosphatases have an enhanced antifungal response to *Candida albicans*. mBio 9(4), e00782–18.

Casadevall A 2022 - Immunity to invasive fungal diseases. Annual Review of Immunology 40, 121–141.

Gaffen S 2017 - IL-17-driven immune signaling in autoimmunity and fungal infections. Blood 130 (Supplement 1): SCI-48.

Ge G, Yang ZY, Li DM, Zhang N et al. 2018 – Distinct host immune responses in recurrent vulvovaginal candidiasis and vulvovaginal candidiasis. Frontiers in Immunology 28(13), 959740.

Govrins M, LassFlörl C. 2023 – *Candida parapsilosis* complex in the clinical setting. Nature Reviews Microbiology 22(1), 46–59.

Guo F, Yang Y, Kang Y, Zang B et al. 2013 – Invasive candidiasis in intensive are units in China: a multicentre prospective observational study. The Journal of antimicrobial chemotherapy 68, 1660–8.

Herculano R, dos Reis C, de Souza S, Brasil G et al. 2024 – Amphotericin B-loaded natural latex dressing for treating *Candida albicans* wound infections using *Galleria mellonella* model. Journal of Controlled Release 365, 744–758.

Hoenigl M, SalmantonGarcía J, Egger M, Gangneux J et al. 2023 – Guideline adherence and survival

of patients with candidaemia in Europe: results from the ECMM *Candida* III multinational European observational cohort study. The Lancet. Infectious diseases 23, 751–761.

Hong N, Lei Y, Chen H, Chen XF et al. 2022 – Genotyping and drug resistance profile of clinical isolates of *Candida albicans* from vulvovaginal candidiasis in the Eastern China. Mycopathologia 187(2), 217–24.

Hou J, Deng J, Liu Y, Zhang W et al. 2022 – Epidemiology, clinical characteristics, risk factors, and outcomes of candidemia in a large tertiary teaching hospital in Western China: a retrospective 5-year study from 2016 to 2020. Antibiotics 11, 788.

Jenks J, Aneke C, AlObaidi M, Egger M et al. 2023 – Race and ethnicity: risk factors for fungal infections? PLoS pathogens 19, e1011025.

Keighley C, Cooley L, Morris AJ, Ritchie D et al. 2021 – Australasian antifungal guidelines steering committee. 2021. Consensus guidelines for the diagnosis and management of invasive candidiasis in haematology, oncology and intensive care settings. Internal Medicine Journal 51, 89–117.

Koehler P, Stecher M, Cornely OA, Koehler D et al. 2019 – Morbidity and mortality of candidaemia in Europe: an epidemiologic meta-analysis. Clinical Microbiology and Infection 10, 1200–12.

Lass-Flörl C, Kanj SS, Govender NP, Thompson III G et al. 2024 – Invasive candidiasis. Nature Reviews Disease Primers 10, 20.

Liao Y, Gao IH, Kusakabe T, Lin WY et al. 2024 - Fungal symbiont transmitted by free-living mice promotes type 2 immunity. Nature 636, 697–704.

Lietz A, Eckel F, Kiss H, Noe-Letschnig M, Farr A. 2023 – Quality of life in women with chronic recurrent vulvovaginal candidosis: a sub-analysis of the prospective multicentre phase IIb/III Prof-001 study. Mycoses 66, 767–773.

Liu C, Luo R, Yi H, Zhang L et al. 2015 – Soil-transmitted helminths in Southwestern China: A cross-sectional study of links to cognitive ability, nutrition, and school performance among children. PLOS Neglected Tropical Diseases 9(6), e0003877.

Liu XF, Ding RR, Yang GM, Qiao YL et al. 2025 – Development and validation of a modified SOFA score for mortality prediction in candidemia patients. Scientific Reports 15, 22044.

Lu H, Hong T, Jiang Y, Whiteway M, Zhang S. 2023 – Candidiasis: From cutaneous to systemic, new perspectives of potential targets and therapeutic strategies. Advanced Drug Delivery Reviews 199, 114960.

Marcos-Zambrano L, Bordallo-Cardona M, Borghi E, Falleni M et al. 2020 – *Candida* isolates causing candidemia show different degrees of virulence in *Galleria mellonella.* Medical mycology 58(1), 83–92.

Mroczyńska M, BrillowskaDąbrowska A. 2021 – virulence of clinical *Candida* isolates. Pathogens 10(4), 466.

Ngamchokwathana C, Chongtrakool P, Waesamaae A, Chayakulkeeree M. 2021 – Risk factors and outcomes of non-*albicans Candida* bloodstream infection in patients with candidemia at Siriraj Hospital: Thailand's largest national tertiary referral hospital. Journal of Fungi 7(4), 269.

Pappas PG, Lionakis MS, Arendrup MC, Ostrosky-Zeichner L, Kullberg BJ. 2018 – Invasive candidiasis. Nature Reviews Disease Primers 4, 18026.

Pfaller MA, Carvalhaes CG, Smith CJ, Diekema DJ et al. 2020 – Bacterial and fungal pathogens isolated from patients with bloodstream infection: frequency of occurrence and antimicrobial susceptibility patterns from the SENTRY Antimicrobial Surveillance Program (2012-2017). Diagnostic Microbiology Infectious Disease 97, 115016.

Pu S, Niu S, Zhang C, Xu X et al. 2017 – Epidemiology, antifungal susceptibilities, and risk factors for invasive candidiasis from 2011 to 2013 in a teaching hospital in Southwest China. Journal of Microbiology, Immunology and Infection 50(1), 97–103.

Ricotta E, Lai Y, Babiker A, Strich J et al. 2020 – Invasive candidiasis species distribution and trends, United States, 2009-2017. The Journal of infectious diseases 223, 1295–1302.

Rottmann B, Singh P, Singh S, Revankar S et al. 2020 – Evaluation of susceptibility and innate immune response in C57BL/6 and BALB/c Mice During *Candida albicans* Endophthalmitis. Investigative ophthalmology visual science 61, 31.

Ruan E, Willem K, Arno H, Jacobus A, Johan L, Carolina H, et al. 2014 – Virulence of South African *Candida albicans* strains isolated from different clinical samples. Medical Mycology 52, 246–253.

Seagle EE, Jackson BR, Lockhart SR, Jenkins EN et al. 2022 – Recurrent candidemia: trends and risk factors among persons residing in four U.S. states, 2011–2018. Open Forum Infectious Diseases. US: Oxford University Press. 9, 545.

Shiori K, Hajime K, Yukio K, Koichi T. 2023 – Clinical features and outcome of persistent candidemia caused by *Candida albicans* versus Non-*albicans Candida* species: A focus on antifungal resistance and follow-up blood cultures. Microorganisms 11(4), 928.

Shuping L, Mpembe R, Mhlanga M, Naicker D et al. 2021 – Epidemiology of culture-confirmed candidemia among hospitalized children in South Africa, 2012-2017. Pediatric Infectious Disease Journal 40, 730–737.

Silvia C, Roberto A, Stefania R, Claudia F et al. 2018 – Epidemiology and risk factors for mortality in bloodstream infection by CP-Kp, ESBL-E, *Candida* and CDI: A single center retrospective study. European Journal of Internal Medicine 48, 44–49.

Sieben RG, Ossa RP, Waack A, Aragon DC et al. 2023 – Risk factors and mortality of candidemia in a children's public hospital in Sao Paulo, Brazil. Revista Argentina de Microbiología 56(3), 281–286.

Simon S, Li R, Andrade JA, Tharian B et al. 2021 ‑ Risk factors for *Candida auris* candidemia: Results from a multicenter case-control study. Open Forum Infectious Diseases 8 (Suppl 1), 454.

Sunil K, Awanish K, Maryam R, Rasoul M et al. 2022 – Overview on the Infections related to rare *Candida* species. Pathogens 11, 963.

Tsai CJY, Loh JMS, Proft T 2016 - *Galleria mellonella* infection models for the study of bacterial diseases and for antimicrobial drug testing. Virulence 7(3), 214–229.

Ulu Kilic A, Alp E, Cevahir F, Ture Z, Yozgat N. 2017 – Epidemiology and cost implications of candidemia, a 6-year analysis from a developing country. Mycoses 60, 198–203.

Verma R, Pradhan D, Hasan Z, Singh H et al. 2021 – A systematic review on distribution and antifungal resistance pattern of *Candida* species in the Indian population. Medical mycology 59, 1145–65.

Weimer KED, Smith PB, Puia-Dumitrescu M, Aleem S. 2021 – Invasive fungal infections in neonates: a review. Pediatric research 91, 404–412.

Xiao M, Sun ZY, Kang M, Guo DW et al. 2018 – Five-year national surveillance of invasive candidiasis: Species distribution and azole susceptibility from the China Hospital Invasive Fungal Surveillance Net (CHIF-NET) study. Journal of Clinical Microbiology, 00577-18.

Xu T, Yi Z, Luo J, Yu H et al. 2019 – Prevalence and trends of transfusion-transmittable infections among blood donors in Southwest China. Journal of Public Health 41(1), 55–61

Zeng Z, Tian G, Ding Y, Yang K et al. 2019 – Surveillance study of the prevalence, species distribution, antifungal susceptibility, risk factors and mortality of invasive candidiasis in a tertiary teaching hospital in Southwest China. BMC Infectious Diseases 19, 939.

Zhang L, Yu SY, Ning YT, X M et al. 2021 – A multicenter retrospective study on the susceptibility of *Candida parapsilosis* and its molecular epidemiology in blood flow separation across the country. Chinese Journal of Mycology 16(05), 289–295.

SUPPLEMENTARY MATERIALS

Molecular identification of clinical isolates by ITS sequencing (Table S1)

Strain identification relying solely on time-of-flight mass spectrometry is inadequate for certain *Candida* species, particularly rare or cryptic strains (e.g., *C. auris*). Since previous reports lacked molecular confirmation, ITS sequencing was used for 65 experimental isolates and 5 *C. auris* in this study to ensure confident species-level identification. Concordance analysis showed 100% agreement between ITS sequencing and TOF-MS results, validating the robustness of strain classification.

Table S1 – Strain validation using both Time-of-flight mass spectrometry (TOF-MS) and ITS molecular sequencing.

Strains	Number	TOF-MS	ITS	Results
C1-C45	45	*C. albicans*	*C. albicans*	Consistent
C46-C50	5	*C. tropicalis*	*C. tropicalis*	Consistent
C51-C55	5	*C. krusei*	*C. krusei*	Consistent
C56-C60	5	*C. parapsilosis*	*C. parapsilosis*	Consistent
C61-C65	5	*N. glabrata*	*N. glabrata*	Consistent
C66-C70	5	*C. auris*	*C. auris*	Consistent

***In vivo* assessment of *Candida* pathogenesis using the *G. mellonella* infection model** (Fig. S1)

After completing *in vitro* virulence phenotyping, the *in vivo* virulence of clinical isolates was further evaluated using the *Galleria mellonella* infection model. The results showed that bloodstream isolates of *C. albicans* caused the fastest mortality, with a median survival time of 78 hours. Mucosal isolates had median survival times ranging from 88 to 104 hours. Among non-*albicans Candida* species, a virulence hierarchy was observed: *C. tropicalis* (101 h) > *C. krusei* (105 h) > *C. parapsilosis* (110 h) > *N. glabrata* (>128 h). The median survival time in the systemic infection models revealed clear virulence stratification among the *Candida* isolates.

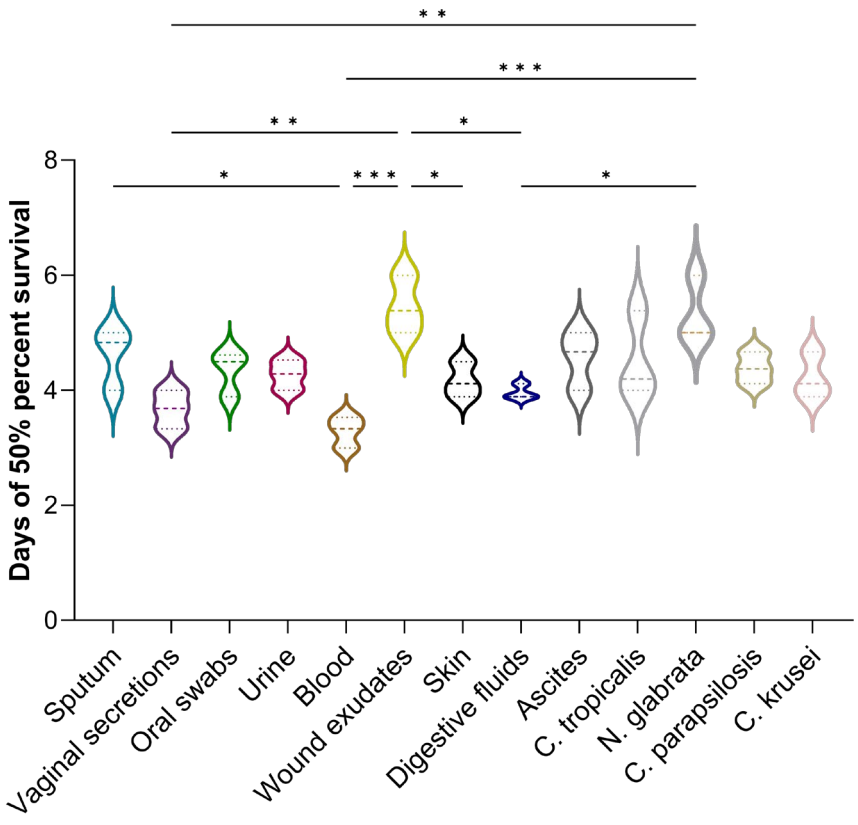

Figure S1 – The median survival time of *Candida* isolates using the *Galleria mellonella* infection model. *G. mellonella* larvae (n=20/group) were injected with 2×10^5 CFU/mL of indicated *Candida* strains to detect the median survival time. Data presented as mean ± SD, ANOVA with Tukey's multiple comparisons (GraphPad Prism 9.0). $^{*}P < 0.0332$, $^{**}P < 0.0021$, $^{***}P < 0.0002$.

Renal histopathological spectrum of *C. albicans* infection (Fig. S2)

On day 4 post-infection, systemic infection with bloodstream-derived *C. albicans* isolates induced severe and diffuse renal pathology, characterized by multifocal microabscesses, extensive tubular epithelial destruction, and dense neutrophilic infiltration (Fig. S2G). Vascular compromise was evident as peritubular hemorrhage and fibrinoid necrosis. Mucosal-derived isolates (from oral and vaginal sources) showed moderate pathogenicity. Oral isolates formed microabscesses with tubular necrosis and neutrophil recruitment, while vaginal isolates induced abscesses, tubular damage (Fig. S2H, S2I). Both mucosal strains predominantly affected the renal cortex without significant extension to the medulla. Wound-secreted isolates exhibited a distinct pattern of corticomedullary destruction, with microabscesses localized in the renal medulla. Isolates from non-sterile anatomical sites displayed reduced renal pathogenicity (Fig. S2B). Digestive fluid and sputum isolates caused mild pelvic inflammation and sparse cortical abscesses (Fig. S2C, S2F). Skin-derived strains and urine isolates triggered perivascular lymphocytic cuffing without invading the renal parenchyma (Fig. S2A, S2D).

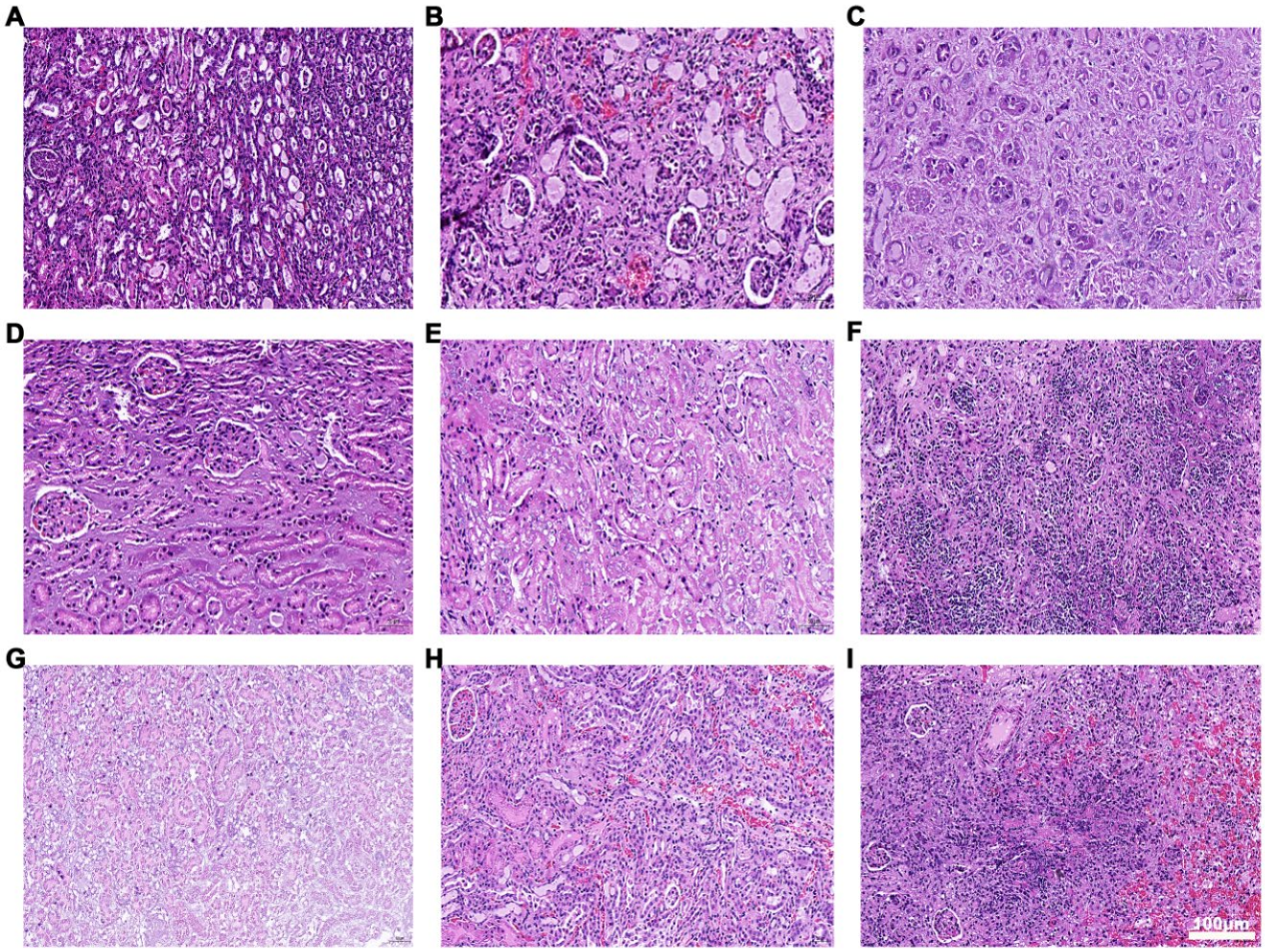

Figure S2 – Renal pathology in *C. albicans*-infected mice (2×10^5 CFU/mL, tail vein injection). H & E staining of kidneys at 4 dpi (20 x). Strains isolated from: (A) Urine, (B) Wound exudates, (C) Digestive fluid, (D) Skin, (E)Ascites, (F) Sputum, (G) Blood, (H) Oral swabs, (I) Vaginal secretions. Scale bar: 100μm.